Photonic and Quantum Waves
https://www.sciltp.com/journals/pqw

Article

Perturbed Dark Optical Solitons

Nicholas J. Ossi [1], Barbara Prinari [1,2], Theodoros P. Horikis [2] and Dimitrios J. Frantzeskakis [3,*]

[1] Department of Mathematics, State University of New York, Buffalo, NY 14260, USA
[2] Department of Mathematics, University of Ioannina, 45110 Ioannina, Greece
[3] Department of Physics, National and Kapodistrian, University of Athens, 15784 Athens, Greece
* Correspondence: dfrantz@phys.uoa.gr

How To Cite: Ossi, N.J.; Prinari, B.; Horikis, T.P.; et al. Perturbed Dark Optical Solitons. *Photonic and Quantum Waves* **2026**, *1*(1), 3.

Received: 7 May 2026
Revised: 8 July 2026
Accepted: 9 July 2026
Published: 20 July 2026

Abstract: We investigate the dynamics of dark optical solitons of the defocusing nonlinear Schrödinger (NLS) equation under the influence of small perturbations. Building on the integrable structure of the unperturbed NLS equation, we present two complementary analytical frameworks: a perturbed conservation-law approach and a linearization-based eigenfunction expansion rooted in inverse scattering theory. Both yield consistent evolution equations for the key soliton parameters—velocity, depth, center and phase—but the eigenfunction approach additionally provides an explicit expression for the first-order correction, from which the structure of the *shelf*, a plateau-like radiation field that inevitably develops around the soliton due to the nonvanishing boundary conditions, can be extracted. It is found that the existence of the shelf is characterized by a single parameter α, which depends on the form of the perturbation. A central result of this work is an exact algebraic relation between the shelf parameter α and the renormalized soliton energy: the rate of energy change is directly and exclusively coupled to α, while all other macroscopic conserved quantities—momentum, Hamiltonian, and center of energy—are shown to decouple from the shelf at leading order. This energy–shelf relation provides a unified and physically transparent accounting of how perturbation energy is partitioned between the soliton core and the radiation it emits. Our analytical results—which are illustrated through several examples of physically relevant perturbations—are consistent with established results in limiting cases. To our knowledge, the energy–shelf relation and the systematic comparison of the two perturbative frameworks within a single, unified treatment are presented here for the first time.

Keywords: dark solitons; defocusing nonlinear Schrödinger equation; perturbation theory; inverse scattering transform; radiation shelf

1. Introduction

Dark solitons are fundamental nonlinear coherent structures supported by the nonlinear Schrödinger (NLS) equation in the normal dispersion regime, or equivalently in the presence of a defocusing nonlinearity. They manifest as localized intensity dips embedded in a stable continuous-wave (cw) background, accompanied by a characteristic phase jump across the point of minimum intensity [1]. In contrast to their bright counterparts, which correspond to localized pulses on a zero background, dark solitons owe their robustness to the modulational stability of the underlying cw state, a property that plays a crucial role in their persistence and dynamics.

Dark solitons were first predicted in the early 1970s in the context of weakly interacting Bose gases [2] and nonlinear optical fibers [3], and were subsequently observed experimentally in nonlinear optical fibers in the late 1980s through a series of pioneering experiments [4–6]. Since then, they have been the subject of extensive theoretical and experimental investigations. Depending on the physical setting, dark solitons can arise either as temporal structures—i.e., localized intensity notches propagating in time along optical fibers—or as spatial entities, corresponding to self-trapped intensity dips in transverse beam profiles in planar waveguides and bulk media. Their unique phase and intensity structure, together with their stability properties, has motivated a range of applications, including all-optical switching, signal processing, and information transmission in fiber-optic communication systems [7–10].

From a theoretical standpoint, the integrability of the unperturbed NLS equation via the inverse scattering transform provides a complete characterization of dark soliton solutions and their interactions. However, ideal integrable conditions are rarely met in realistic physical systems. In practice, optical media exhibit a variety of higher-order and non-ideal effects that perturb the NLS dynamics. These include linear and nonlinear losses, gain mechanisms, higher-order dispersion, diffusion, self-steepening, Raman scattering, and other dissipative or conservative contributions [7–10]. Even weak perturbations can induce significant cumulative effects over long propagation distances, leading to phenomena such as soliton acceleration, deformation, radiation emission, and eventual decay. However, it should be pointed out that perturbation methods that have been developed for the study of dark solitons under such perturbations may typically involve more complications than those developed for bright solitons [11]. This is due to the nonhomogeneous boundary conditions associated with dark solitons: indeed, perturbation-induced dark soliton dynamics involves both the evolution of the background and the evolution of the soliton itself.

Various approaches have been used in the past for the study of perturbed dark optical solitons. Earlier works have been devoted to the effect of linear loss—see [12] for numerical and [13,14] for analytical investigations, where the evolution of the background amplitude and soliton depth were determined. Later, it was shown [15] that the evolution of the background was independent of the soliton, and the asymptotic behavior at infinity was used to separate the propagation of the background magnitude from the soliton "core"; in the same work [15], the soliton's amplitude/width was determined in the framework of the Hamiltonian approach of the perturbation theory for dark solitons (this approach has also been extensively used in studies on dark solitons in Bose-Einstein condensates [16,17]). On the other hand, another class of perturbative approaches relies on the Inverse Scattering Transform (IST) [18]. In particular, it was shown [19] that orthogonality conditions derived from a set of squared Jost functions (eigenfunctions of the linearized NLS operator [20]) may lead to the determination of the soliton parameters. Later, other contributions [21–24] offered various corrections and modifications to the details of this IST-based approach. Notice that in the above works, the emergence of a radiation field, in the form of a plateau-shaped linear wave—referred to as *shelf* [25]—that develops around a perturbed dark soliton, was not taken into account. Nevertheless, shelves are developed around dark solitons under external perturbations [26], and can be used to explain discrepancies in the perturbed conservation laws—see also relevant discussion in Refs. [11,25] for the Korteweg-de Vries (KdV) equation.

In the present work, we investigate the dynamics of dark solitons within the framework of the defocusing NLS equation subject to perturbations. Our goal is to develop a systematic analytical description of how such perturbations affect the key soliton parameters, including amplitude (or depth), velocity, and phase structure, as well as to quantify the generation of dispersive radiation. We employ two different analytical approaches. The first one is a multiscale expansion method, combined with the use of perturbed conservation laws [27], which has been used in studies on dark soliton dynamics under various perturbations [28,29]. The second approach, which was devised very recently [30], is an eigenfunction-expansion-based perturbation theory for the defocusing NLS; after briefly presenting both approaches, we provide a number of applications concerning physically relevant perturbations of dark optical solitons (see, e.g., [8,10,15]); these include linear and nonlinear damping, self-steepening effect, higher-order dispersion, and stimulated Raman scattering. Both approaches provide identical results concerning the slow-time evolution of the dark soliton parameters. Special emphasis is placed on the radiation shelf emerging on the soliton sides, which is found to be directly connected with the rate of change of the soliton energy. Our results provide a deeper insight into the effects of perturbations, which is essential for assessing the robustness of dark solitons in realistic optical systems, as well as for guiding their practical utilization in applications where deviations from ideal integrability cannot be neglected.

It is useful, at this point, to delineate explicitly what is drawn from earlier work and what is new here. The perturbed conservation-law formalism of Section 2 follows the framework established in Ref. [27] and subsequently employed in Refs. [28,29], while the eigenfunction-expansion formalism of Section 3—including the squared-eigenfunction basis, the completeness relation, and the integral representation of the first-order correction—was developed in the recent work [30]. Likewise, the individual results for linear damping, self-steepening, and higher-order dispersion that appear among our examples have, in various forms, been reported previously [27,28,30]. The novel contributions of the present work are the following: (i) a unified, side-by-side comparison of the two perturbative approaches, demonstrating explicitly that they yield identical evolution equations for the background, depth, and velocity, and identifying the soliton center as the single parameter for which the two predictions differ; (ii) the exact algebraic energy-shelf relation $E_Z = -(\alpha - 2B_Z)$, which couples the rate of change of the renormalized soliton energy directly and exclusively to the shelf parameter α; and (iii) the accompanying analysis (Section 4.5) showing that the remaining macroscopic conserved quantities—momentum, Hamiltonian, and center of energy—decouple from α at leading order, together with the new results for higher-order dissipation and stimulated

Raman scattering, which were not treated in the references above. These contributions provide a single, physically transparent accounting of how perturbation energy is partitioned between the soliton core and its radiation.

Our presentation is organized as follows. First, we present our analytical approaches, namely the method of perturbed conservation laws (Section 2), and the linearization and eigenfunction expansion technique (Section 3). In Section 4 we apply the results of our methodologies to study the effect of typical perturbations on optical dark solitons and analyze the emergence and the physical significance of the radiation shelf. Finally, in Section 5 we summarize our findings.

2. Perturbed Conservation Laws

We consider an NLS equation in the normal dispersion regime (defocusing NLS), which incorporates an additional small perturbation term; the model under consideration can be expressed in dimensionless form as (see, e.g., Ref. [10]):

$$iU_z - \frac{1}{2}U_{tt} + |U|^2U = \varepsilon F[U], \qquad 0 < \varepsilon \ll 1. \tag{1}$$

Here, $U(t,z)$ is the complex electric field envelope, t is time (in a reference frame moving with the group velocity), z is the propagation distance, and $\varepsilon F[U]$ is a small perturbation. Equation (1) is supplemented with non-vanishing boundary conditions as $t \to \pm\infty$:

$$U^{\pm}(z) = \lim_{t\to\pm\infty} U(t,z).$$

As shown in [27], the background evolves independently of any localized disturbance, and in particular the background amplitude $U^{\pm}$ satisfies the equation:

$$\frac{d}{dz}|U^{\pm}| = \varepsilon\, \mathrm{Im}\, F[|U^{\pm}|], \tag{2}$$

for any perturbation that preserves the phase symmetry of the NLS equation, namely the following condition holds: $F[U(z,t)e^{i\theta}] = F[U(z,t)]e^{i\theta}$, at least asymptotically (i.e., in the limits $t \to \pm\infty$). This provides a sufficient condition to keep the magnitude of the background equal on either side for all z whenever it starts equal, namely if, at $z = 0$, $|U^+(0)| = |U^-(0)|$ then $|U^+(z)| = |U^-(z)| \equiv u_\infty(z)$. It is therefore convenient to factor out the fast evolution of the background phase by letting:

$$U = u \exp\left[i\int_0^z u_\infty^2(s)ds\right],$$

and write the perturbed NLS equation in the form:

$$iu_z - \frac{1}{2}u_{tt} + \big(|u|^2 - u_\infty^2\big)u = \varepsilon F[u], \qquad 0 < \varepsilon \ll 1, \tag{3}$$

so that $u_\infty(Z)$, with $Z = \varepsilon z$ the slow evolution variable, denotes the slowly varying background amplitude. Then, as $t \to \pm\infty$ one has $u \to u_\infty e^{i\phi^{\pm}}$, and $u_\infty > 0$ evolves according to:

$$\frac{d}{dZ}u_\infty = \mathrm{Im}\big[F[u_\infty]\big]. \tag{4}$$

This is what distinguishes dark solitons from their bright counterparts, and is the source of all the essential complications in the perturbation theory. It is also important to point out that the total phase difference $\Delta\phi_\infty = \phi^+ - \phi^-$, which is related to the depth of the dark soliton, satisfies $d(\Delta\phi_\infty)/dZ = 0$ and is therefore an exact invariant of the perturbed system. This separation of the background dynamics from the soliton core is one of the structural pillars of the entire method.

In the unperturbed case ($\varepsilon = 0$), the NLS (3) possesses the dark soliton solution

$$u_s(t,z) = \big(A + iB\tanh[B(t - Az - t_0)]\big)e^{i\sigma_0}, \tag{5}$$

which satisfies the boundary conditions

$$\lim_{t\to\pm\infty} u_s = u_\infty e^{i\sigma_0 \pm i\theta}, \quad u_\infty^2 = A^2 + B^2, \quad \theta = \arg(A + iB). \tag{6}$$

In (5), the soliton parameters, A, B, t_0, σ_0, are all real. The parameters A and B denote the velocity and amplitude (i.e., the depth of the intensity dip) of the soliton, respectively. The parameters t_0 and σ_0 represent the initial location of the soliton center and phase of the soliton, respectively. Notice that for $A = 0$ the soliton is a stationary—so called "black"—soliton, with a π phase difference, while for $A \neq 0$, the dark soliton is a moving—so called "gray"—soliton, with a phase difference $2\tan^{-1}(B/A)$.

In the perturbed case ($\varepsilon \neq 0$), we write $u = q\,e^{i\phi}$ with $q > 0$ and ϕ real. Strictly bounding $q > 0$ restricts our focus on gray solitons ($A \neq 0$); for black solitons ($A = 0$), q can smoothly pass through zero and become negative to account for the π phase jump. In the framework of the method of multiple scales, we introduce the slow variable $Z = \varepsilon z$, and assume that the soliton parameters, A, B, t_0, σ_0, are functions of Z. Then we introduce the asymptotic expansions

$$q(Z, z, t) = q_0 + \varepsilon q_1 + O(\varepsilon^2), \quad \phi(Z, z, t) = \phi_0 + \varepsilon\phi_1 + O(\varepsilon^2),$$

into (3), we find that, at the leading order, $O(\varepsilon^0)$, the resulting equations for q_0 and ϕ_0 are satisfied by the exact gray soliton solution (5). Specifically, in the co-moving frame $\tau = t - \int_0^z A(\varepsilon s)\,ds - t_0(Z)$, where $A(Z)$ is the soliton velocity and $t_0(Z)$ is the soliton center, the leading-order solution reads

$$q_0 = \sqrt{A^2 + B^2\tanh^2(B\tau)}, \quad \phi_0 = \tan^{-1}\left[\frac{B}{A}\tanh(B\tau)\right] + \sigma_0(Z), \tag{7}$$

where $\sigma_0(Z)$ is a slowly varying global phase and the parameters satisfy the background constraint $A^2 + B^2 = u_\infty^2$. The phase jump across the soliton core is given by

$$\Delta\phi_0 = 2\tan^{-1}\left(\frac{B}{A}\right), \quad A = u_\infty\cos\left(\frac{\Delta\phi_0}{2}\right), \quad B = u_\infty\sin\left(\frac{\Delta\phi_0}{2}\right). \tag{8}$$

The four slowly varying core parameters, A, B, t_0, σ_0, remain to be determined at the next orders of approximation.

At order $O(\varepsilon)$, the equations for q_1 and ϕ_1 are linear and inhomogeneous. A stationary solution is sought in the moving frame. The critical qualitative feature that emerges at this stage is that q_1 and $\phi_{1\tau}$ do not decay as $\tau \to \pm\infty$; instead, they asymptotically approach distinct nonzero constants,

$$q_1 \;\to\; q_1^{\pm}(Z), \quad \phi_{1\tau} \;\to\; \phi_{1\tau}^{\pm}(Z) \quad \text{as } \tau \to \pm\infty. \tag{9}$$

This results in the *shelf*, a plateau-like deformation extending away from the soliton. The shelf is an unavoidable structural feature forced by the nonvanishing boundary conditions: any perturbation drives a mean shift in the amplitude and a linearly growing contribution to the phase away from the soliton core. Because the approximate inner solution does not match the outer boundary condition at infinity, a boundary layer must be introduced.

To analyze this boundary layer, one linearizes Equation (3) around the background u_∞ and expresses u as

$$u \approx (u_\infty + \varepsilon w)\exp[i(\phi^{\pm} + \varepsilon\vartheta)].$$

At the leading order, the boundary layer is independent of the perturbation F. The resulting equations for w and ϑ are governed by a linear wave equation, of the linearized Boussinesq type, characterized by the dispersion relation

$$\omega^2 = u_\infty^2(Z)\,k^2 + \frac{1}{4}k^4. \tag{10}$$

In the long-wavelength limit, $|k| \ll 1$, this reduces to $\omega \approx \pm u_\infty(Z)\,k$, so the shelf edges propagate away from the soliton with instantaneous speed $\pm u_\infty(Z)$ in the stationary frame. In the co-moving frame τ, the relative speeds of the left and right wavefronts are $-u_\infty - A$ and $+u_\infty - A$. Integrating these relative velocities yields the positions of the expanding shelf boundaries:

$$S_L(z) = -\int_0^z \big[u_\infty(\varepsilon s) + A(\varepsilon s)\big]\,ds, \quad S_R(z) = \int_0^z \big[u_\infty(\varepsilon s) - A(\varepsilon s)\big]\,ds. \tag{11}$$

Since $A \leq u_\infty$, the soliton core can never overtake the shelf. The precise transition from the inner quasi-stationary region to the outer equilibrium is obtained via the similarity variable $\xi = x/z^{1/3}$, yielding Airy-type solutions that confirm the shelf edges are smooth dispersive fronts matched to the limits (9).

The perturbed conservation laws of (3) provide the evolution equations for the soliton parameters. Because the first-order correction is non-decaying, integrals must be evaluated over the expanding inner region $[S_L(z), S_R(z)]$, with shelf contributions entering explicitly through the moving boundaries. The relevant *renormalized*—so that the pertinent integrals are finite—conserved quantities are the energy E, the momentum I, the center of energy R, and the Hamiltonian H, given by [8,15,16]:

$$\begin{aligned} E &= \int_{-\infty}^{\infty} (u_\infty^2 - |u|^2)\, dt\,, &\text{(12a)}\\ I &= \frac{i}{2}\int_{-\infty}^{\infty} (u\, u_t^* - u^*\, u_t)\, dt - u_\infty^2 \mathrm{Arg}(u)\Big|_{-\infty}^{+\infty}\,, &\text{(12b)}\\ R &= \int_{-\infty}^{\infty} t(u_\infty^2 - |u|^2)\, dt\,, &\text{(12c)}\\ H &= \int_{-\infty}^{\infty} \left[\frac{1}{2}|u_t|^2 + \frac{1}{2}(u_\infty^2 - |u|^2)^2\right] dt. &\text{(12d)} \end{aligned}$$

Evaluating these balances at leading order, applying the fundamental theorem of calculus to handle the moving boundaries, and using the explicit soliton form (7), one arrives at the following closed system. From the Hamiltonian balance,

$$2B\,\frac{dA}{dZ} = \mathrm{Re}\int_{-\infty}^{\infty} F[u_0]\, u_{0\tau}^*\, d\tau. \tag{13}$$

From the energy and momentum balances,

$$B_Z - u_\infty\big[(u_\infty - A)q_1^+ + (u_\infty + A)q_1^-\big] = \mathrm{Im}\int_{-\infty}^{\infty} \big(F[u_\infty]u_\infty - F[u_0]u_0^*\big)\, d\tau, \tag{14}$$

$$2(AB)_Z + u_\infty^2\big[(u_\infty - A)\phi_{1\tau}^+ + (u_\infty + A)\phi_{1\tau}^-\big] = -2\,\mathrm{Re}\int_{-\infty}^{\infty} F[u_0]\, u_{0\tau}^*\, d\tau. \tag{15}$$

Taking the limit $\tau \to \pm\infty$ in the first-order phase equation yields the asymptotic matching condition,

$$A\,\phi_{1\tau}^\pm + 2u_\infty q_1^\pm = \phi_Z^\pm \pm \frac{1}{2}\,(\Delta\phi_0)_Z + \sigma_{0Z}, \tag{16}$$

where $\phi_Z^\pm = -\mathrm{Re}[F[u_\infty]]/u_\infty$ is known from (4). Together, these form a closed algebraic system for the six unknowns $q_1^\pm$, $\phi_{1\tau}^\pm$, A_Z, and σ_{0Z}. The complete solution of the system is

$$\begin{aligned} \frac{d}{dZ}u_\infty &= \mathrm{Im}[F[u_\infty]], &\text{(17a)}\\ 2B\,\frac{dA}{dZ} &= \mathrm{Re}\int_{-\infty}^{\infty} F[u_0]\, u_{0\tau}^*\, d\tau, &\text{(17b)}\\ u_\infty\,\frac{d\sigma_0}{dZ} &= B_Z - \mathrm{Im}\int_{-\infty}^{\infty}\big(F[u_\infty]u_\infty - F[u_0]u_0^*\big)\, d\tau + \mathrm{Re}[F[u_\infty]], &\text{(17c)}\\ q_1^+ &= \frac{\sigma_{0Z} + \frac{1}{2}(\Delta\phi_0)_Z}{2(u_\infty - A)}, &\text{(17d)}\\ q_1^- &= \frac{\sigma_{0Z} - \frac{1}{2}(\Delta\phi_0)_Z}{2(u_\infty + A)}, &\text{(17e)}\\ \phi_{1\tau}^+ &= -2q_1^+, \qquad \phi_{1\tau}^- = \quad 2q_1^-, &\text{(17f)}\\ B_Z &= \frac{u_\infty u_{\infty Z} - AA_Z}{B}, &\text{(17g)}\\ (\Delta\phi_0)_Z &= \frac{2AB_Z - 2BA_Z}{u_\infty^2}. &\text{(17h)} \end{aligned}$$

Equation (17c) is particularly noteworthy: it shows that σ_0 evolves nontrivially, meaning the soliton accumulates a phase at a rate different from that of the cw background on which it rides. Furthermore, the total phase change across the inner region, $\Delta\phi_0 + \varepsilon\,\Delta\phi_1$, is exactly conserved, meaning the evolving core phase jump is precisely compensated by the phase carried by the shelf.

The remaining parameter, the soliton position $t_0(Z)$, cannot be extracted from the conservation laws. Instead, one must work directly with the first-order correction term. We thus look for a solution of the perturbed NLS (3) in the form of the asymptotic expansion

$$u = u_0 + \varepsilon u_1 + O(\varepsilon^2).$$

Then, at $O(\varepsilon)$, and in the moving frame, we find that a stationary solution for u_1 satisfies the coupled real system $\mathcal{L}\,U_1 = G[u_0]$, where $\mathcal{L}$ is the linearization of the NLS operator about the gray soliton. A particular solution u_{1p} is obtained by variation of parameters, where the contribution of t_{0Z} appears linearly and explicitly. Matching the asymptotic behavior of u_1 to the shelf limits fixes the homogeneous coefficients. Then, substituting the full form of u_1 into the Hamiltonian evolution equation at order $O(\varepsilon^2)$ yields a well-posed second-order ODE for $t_0(Z)$.

In summary, the perturbation theory for gray dark solitons is intrinsically nonlocal, requiring regularized conservation laws to remain finite. The soliton core, the surrounding shelf, and the evolving background form a tightly coupled system whose dynamics cannot be disentangled. The conservation laws receive shelf contributions through the moving boundaries S_L and S_R; the shelf amplitudes are driven by the slow evolution of the core parameters; and the soliton position requires solving the full first-order linearized problem. However, a striking elegance of this method is that the amplitude, velocity, and global phase dynamics only require asymptotic limits of the shelf, successfully sidestepping the need for complete higher-order inner solutions. This structure stands in sharp contrast to bright soliton perturbation theory, where decaying boundary conditions confine the perturbation near the core and Fredholm alternatives on a fixed domain suffice. For dark solitons, neglecting the expanding shelf leads to an inconsistent scheme.

3. Linearization and Eigenfunction Expansion

An alternative approach to analytically characterize the dynamics of dark solitons subject to small perturbations is to linearize the perturbed NLS equation about an exact dark soliton solution and identify a natural basis of eigenfunctions of the linearization operator. The relevant complete basis of eigenfunctions is crucially tied to the integrability of the NLS equation. After performing an eigenfunction expansion of the linearized problem, it is possible to obtain not only the evolution equations governing the soliton parameters but also an explicit, though complicated, expression for the first-order term in the perturbation expansion. Moreover, this expression for the first-order correction can be used to extract useful information about the propagating shelf that can develop around the soliton as a result of the perturbation. The construction of the squared-eigenfunction basis, the completeness relation (21), and the integral representation (30) of the first-order correction are due to Ref. [30]; we summarize them here only to the extent needed to make the present paper self-contained, and refer the reader to that work for the full derivation. Our purpose in reproducing this material is to place it side by side with the conservation-law approach of Section 2 and, in Section 4.5, to derive from it the energy-shelf relation and the decoupling of the remaining conserved quantities, which constitute the new results of this paper.

As mentioned above, for $\varepsilon = 0$, the defocusing NLS (3) admits the exact dark soliton solution (5). In the case $\varepsilon \neq 0$, the perturbation-induced dynamics of a dark soliton can be studied as follows. First, as before, we allow the soliton's core parameters to depend on the slow evolution variable $Z = \varepsilon z$, namely $A = A(Z)$, $B = B(Z)$, $\sigma_0 = \sigma_0(Z)$ and $t_0 = t_0(Z)$, and consider the ansatz

$$u(t,z) = e^{i\sigma_0}\left[u_s(\tau) + \varepsilon\tilde{u}(\tau,z) + O(\varepsilon^2)\right], \tag{18}$$

with $\tau = t - \int_0^z A(\varepsilon s)\,ds - t_0(Z)$. Note that in contrast to the approach in the previous Section, here we expand the complex valued function u rather than expanding the modulus and phase separately. Obviously the two expansions are equivalent, and in particular for the leading order solution one has

$$q_0 = |u_s|, \qquad \phi_0 = \arg(u_s) + \sigma_0.$$

Substituting (18) into (3) yields the linearized problem

$$(i\partial_z + L)U(\tau,z) = W(\tau), \qquad U = \begin{bmatrix}\tilde{u}\\ \tilde{u}^*\end{bmatrix}, \qquad W = \begin{bmatrix} w[u_s] \\ -w[u_s]^*\end{bmatrix}, \tag{19a}$$

$$w[u_s] = F_0 - ie^{-i\sigma_0}\partial_Z(u_s e^{i\sigma_0}), \qquad F_0 = e^{-i\sigma_0}F[u_s e^{i\sigma_0}], \tag{19b}$$

where the linearization operator is

$$L = \begin{bmatrix} -\frac{1}{2}\partial_\tau^2 - iA\partial_\tau + (2|u_s(\tau)|^2 - u_\infty^2) & u_s(\tau)^2 \\ -u_s^*(\tau)^2 & \frac{1}{2}\partial_\tau^2 - iA\partial_\tau - (2|u_s(\tau)|^2 - u_\infty^2) \end{bmatrix}. \tag{20}$$

Note that the above linearization operator L is analogous to the pertinent one, denoted by $\mathcal{L}$, mentioned at the end of Section 2. However, these operators are not identical, since in [27] the linearized problem is written in terms of the real and imaginary parts of the first-order correction. Now, we need to identify the natural basis in which to expand the first-order correction U and the inhomogeneous term W in (19a). In [30], it was shown that the operator L possesses a complete basis of eigenfunctions, satisfying a closure/completeness relation of the form:

$$2\pi\delta(\tau-\tau')I = \fint_{-\infty}^{\infty} \frac{\zeta}{2\lambda(\zeta)|\zeta-\zeta_1|^4} \mathcal{Z}(\tau,\zeta)\Upsilon(\tau',\zeta)^T d\zeta + \frac{\pi\zeta_1}{4B^3}\Big[\mathcal{Z}_1(\tau)\tilde{\Upsilon}_1(\tau')^T + \tilde{\mathcal{Z}}_1(\tau)\Upsilon_1(\tau')^T\Big]. \tag{21}$$

In (21), the symbol $\fint$ denotes the Cauchy principal value integral. Importantly, $\lambda(\zeta) = (\zeta - u_\infty^2\zeta^{-1})/2$ has zeros at $\zeta = \pm u_\infty$, and as such the above principal value integral has simple poles at those points. The continuous eigenfunctions $\{\mathcal{Z}(\tau,\zeta), \zeta \in \mathbb{R}\}$ and discrete eigenfunctions $\{\mathcal{Z}_1(\tau), \tilde{\mathcal{Z}}_1(\tau)\}$ and their respective adjoints $\{\Upsilon(\tau,\zeta), \zeta \in \mathbb{R}\}$ and $\{\tilde{\Upsilon}_1(\tau), \Upsilon_1(\tau)\}$ are known as *squared eigenfunctions*. They are quadratic combinations of the Jost eigenfunctions of the inverse scattering transform associated with the defocusing NLS equation with nonzero boundary conditions (see Ref. [31] for a review). Full details on the squared eigenfunctions and their completeness are given in [30]. Physically, this basis cleanly separates the two channels through which a perturbation can act on the soliton. The discrete eigenfunctions $\{\mathcal{Z}_1, \tilde{\mathcal{Z}}_1\}$ are localized about the soliton core and encode deformations of the soliton parameters themselves—depth, velocity, center, and phase—whereas the continuous eigenfunctions $\{\mathcal{Z}(\tau,\zeta)\}$ represent the radiation modes of the background. The simple poles of the completeness relation at $\zeta = \pm u_\infty$, i.e., the branch points of the continuous spectrum, sit precisely at the edge separating these two channels; as we show below, it is the residue at these poles that controls the slow leakage of energy from the core into the long-lived radiation plateau, the shelf. For the purpose of the present discussion, we simply invoke the completeness relation (21), which allows one to expand any function $f(\tau)$ in the following way:

$$f(\tau) = \frac{1}{2\pi}\fint_{-\infty}^{\infty} \frac{\zeta}{2\lambda(\zeta)|\zeta-\zeta_1|^4}\langle\Upsilon(\zeta), f\rangle \mathcal{Z}(\tau,\zeta)d\zeta + \frac{\zeta_1}{8B^3}\Big[\langle\tilde{\Upsilon}_1, f\rangle\mathcal{Z}_1(\tau) + \langle\Upsilon_1, f\rangle\tilde{\mathcal{Z}}_1(\tau)\Big], \tag{22}$$

where the inner product is defined by $\langle g, f\rangle = \int_{-\infty}^{\infty} g(\tau')^T f(\tau')d\tau'$. All quantities necessary to perform the above expansion are known explicitly as follows. The continuous eigenfunctions are given by

$$\mathcal{Z}(\tau,\zeta) = \begin{bmatrix} [i\zeta_1\zeta^{-1}(\zeta-\zeta_1^*) + Be^{-B\tau}\operatorname{sech}(B\tau)]^2 \\ [(\zeta-\zeta_1^*) - iBe^{-B\tau}\operatorname{sech}(B\tau)]^2 \end{bmatrix} e^{2i\lambda(\zeta)\tau}, \tag{23a}$$

$$\Upsilon(\tau,\zeta) = \begin{bmatrix} -[i\zeta_1^*\zeta^{-1}(\zeta-\zeta_1) - Be^{-B\tau}\operatorname{sech}(B\tau)]^2 \\ [(\zeta-\zeta_1) + iBe^{-B\tau}\operatorname{sech}(B\tau)]^2 \end{bmatrix} e^{-2i\lambda(\zeta)\tau}, \tag{23b}$$

and the discrete eigenfunctions are given by

$$\mathcal{Z}_1(\tau) = B^2\begin{bmatrix} 1 \\ -1 \end{bmatrix}\operatorname{sech}^2(B\tau), \qquad \Upsilon_1(\tau) = -B^2\begin{bmatrix} 1 \\ 1 \end{bmatrix}\operatorname{sech}^2(B\tau), \tag{24}$$

$$\tilde{\mathcal{Z}}_1(\tau) = \mathcal{Z}_1'(\tau) - \frac{2iB}{\zeta_1}\begin{bmatrix} -u_s(\tau) \\ u_s^*(\tau) \end{bmatrix}, \qquad \tilde{\Upsilon}_1(\tau) = \Upsilon_1'(\tau) - \frac{2iB}{\zeta_1}\begin{bmatrix} u_s^*(\tau) \\ u_s(\tau) \end{bmatrix}, \tag{25}$$

with

$$\mathcal{Z}_1'(\tau) = -2iB\left\{\begin{bmatrix} u_\infty^2\zeta_1^{-2} \\ -1 \end{bmatrix} e^{-B\tau}\operatorname{sech}(B\tau) - AB\zeta_1^{-1}\begin{bmatrix} 1 \\ -1 \end{bmatrix}\tau\operatorname{sech}^2(B\tau)\right\}, \tag{26a}$$

$$\Upsilon_1'(\tau) = 2iB\left\{\begin{bmatrix} u_\infty^2\zeta_1^{-2} \\ 1 \end{bmatrix} e^{B\tau}\operatorname{sech}(B\tau) + AB\zeta_1^{-1}\begin{bmatrix} 1 \\ 1 \end{bmatrix}\tau\operatorname{sech}^2(B\tau)\right\}. \tag{26b}$$

In the above,

$$\zeta_1 = A + iB, \quad \lambda(\zeta) = \frac{1}{2}(\zeta - u_\infty^2\zeta^{-1}), \quad \lambda(\zeta_1) = iB, \quad k(\zeta) = \frac{1}{2}(\zeta + u_\infty^2\zeta^{-1}), \quad k(\zeta_1) = A. \tag{27}$$

Moreover, the eigenfunctions in the completeness relation satisfy:

$$L\mathcal{Z}(\tau,\zeta) = -2\lambda(\zeta)\big(k(\zeta) - A\big)\mathcal{Z}(\tau,\zeta), \qquad L\mathcal{Z}_1(\tau) = 0, \qquad L\tilde{\mathcal{Z}}_1(\tau) = 2B^2\zeta_1^{-1}\mathcal{Z}_1(\tau). \tag{28}$$

Performing an eigenfunction expansion of the quantities in (19a), using (28), and equating coefficients, we find that necessary conditions to prevent secular growth are

$$\langle \Upsilon_1, W\rangle = \langle \tilde{\Upsilon}_1, W\rangle = 0, \tag{29}$$

and an explicit expression for the first-order term in the perturbation expansion is

$$U(\tau, z) = -\frac{1}{2\pi}\fint_{-\infty}^{\infty} \frac{\zeta}{|\zeta-\zeta_1|^4} \frac{1-e^{-2i\lambda(\zeta)(k(\zeta)-A)z}}{4\lambda(\zeta)^2\big(k(\zeta)-A\big)} \langle \Upsilon(\zeta), W\rangle \mathcal{Z}(\tau,\zeta)\, d\zeta. \tag{30}$$

This explicit representation of the first-order correction is a notable advantage of the present method. Note that since $\lambda(\pm u_\infty) = 0$, the first-order correction generically possesses simple poles at $\zeta = \pm u_\infty$, which are the reason for the generation of a propagating shelf around the perturbed soliton. Analyzing the first-order correction shows that the shelf emerges if and only if $\alpha \neq 0$, where

$$\alpha := -i\left\langle \begin{bmatrix} u_s^* \\ u_s \end{bmatrix}, W \right\rangle = 2\int_{-\infty}^{\infty} \left\{ \mathrm{Im}\left[u_s^* F_0\right] - u_\infty u_{\infty Z} \right\} d\tau + 2B_Z. \tag{31}$$

The physical content of α is transparent: it is the projection of the perturbation W onto the generalized discrete eigenmode of L, and therefore measures the net rate at which the perturbation pumps amplitude into the radiative channel rather than into a simple reshaping of the soliton core. When this projection vanishes the perturbation is entirely absorbed by the core parameters and no shelf forms; when it does not, the excess is shed symmetrically into the two plateaus flanking the soliton. This is the precise sense in which α acts as the single scalar order parameter for shelf formation, and it is what makes the energy budget discussed in Section 4.5 so compact. In particular, the principal value integral (30) can be studied asymptotically for large $|\tau|$. In this limit, due to the rapidly oscillating factor in $\mathcal{Z}$, the primary contributions to the integral come from the poles. Performing this asymptotic evaluation shows that the integral is only non-negligible in the interval $-(u_\infty + A) < \tau < (u_\infty - A)$, which corresponds to the shelf region, and within this region the height and phase gradient of the shelf on either side of the soliton are given by

$$h^{\pm} = \frac{\alpha(u_\infty \pm A)}{4u_\infty B^2}, \qquad \varphi_\tau^{\pm} = \mp 2h^{\pm}. \tag{32}$$

If $\alpha = 0$, the poles at $\zeta = \pm u_\infty$ in the first-order correction are removed and there is no shelf. Additionally, in all cases where a shelf develops, there is inevitable secular growth in the first-order correction integral that can be suppressed by choosing

$$\frac{d\sigma_0}{dZ} = \frac{\alpha}{2u_\infty}, \tag{33}$$

which serves as a generic formula for the evolution of the soliton phase. The first orthogonality condition yields a formula for the soliton velocity:

$$\langle \Upsilon_1, W\rangle = 0 \implies \frac{dA}{dZ} = \frac{B}{2}\,\mathrm{Im}\int_{-\infty}^{\infty} F_0\,\mathrm{sech}^2(B\tau)\, d\tau. \tag{34}$$

The second orthogonality condition can be written in terms of α:

$$\langle \Upsilon_1', W\rangle + \frac{2B\alpha}{\zeta_1} = 0. \tag{35}$$

The inner product $\langle \Upsilon_1', W\rangle$, where the generalized discrete eigenmode Υ_1' is given in (26b), is generically divergent. This proves to be helpful, as in this case (35) provides two conditions on the soliton parameters—one to remove the divergence and another to set the convergent terms to zero. In practice, the condition to remove the divergence provides the evolution of the depth parameter B or the background u_∞, which are not independent. The other one can be obtained through

$$u_\infty \frac{du_\infty}{dZ} = A\frac{dA}{dZ} + B\frac{dB}{dZ}. \tag{36}$$

Finally, the second condition that results from (35) can be used to determine a prediction for the evolution of the soliton center t_0.

To summarize, if $\alpha \neq 0$, with α as in (31), a propagating shelf develops around the soliton with approximate height and phase gradient given by (32) and the soliton phase evolves according to (33). If $\alpha = 0$, no shelf develops and the soliton phase does not evolve independently of the background phase. The orthogonality conditions (29) then provide three conditions from which the rest of the soliton parameters can be determined. In [30], it was found that the predictions for the evolution of the background u_∞, velocity A, and depth B hold up well for propagation distances of order $z \sim 1/\varepsilon$ and beyond. On the other hand, the predictions for the soliton phase σ_0 and center t_0 obtained using this approach do not necessarily remain valid as long, though they do accurately capture the small z behavior. As explained in [30], in order to obtain estimates for the soliton phase and center which hold up to $z = O(1/\varepsilon)$, one would likely have to determine the $O(\varepsilon^2)$ corrections for the amplitude and velocity. This is consistent with the approach in [27] for determining the soliton center t_0, briefly summarized at the end of Section 2, where the Hamiltonian evolution equation at order $O(\varepsilon^2)$ was used. On the other hand, we stress that the predictions for the soliton phase are similarly affected, and obtaining estimates for the soliton phase accurate up to $z = O(1/\varepsilon)$ is currently an open problem.

4. Optical Perturbations and Emergence of the Shelf

Let us now proceed with the presentation of several examples, where physically relevant perturbations (see, e.g., Refs. [8,10,15]) are considered, and the perturbation-induced dynamics of optical dark solitons is studied by means of the approaches presented in the previous Sections. Furthermore, we will elaborate on the emergence of the shelf, which will be connected with the conservation of energy.

4.1. Linear and Nonlinear Damping

In the case of a linear damping perturbation,

$$F[u] = -iu, \tag{37}$$

the background, velocity, and depth parameters decay exponentially with Z,

$$u_\infty(Z) = u_\infty(0)e^{-Z}, \qquad A(Z) = A(0)e^{-Z}, \qquad B(Z) = B(0)e^{-Z}. \tag{38}$$

These predictions follow from either the approach of Section 2 or that of Section 3. Now, according to the approach of Section 3, the shelf parameter α is found from (31) to be

$$\alpha = 2B, \tag{39}$$

which indicates the development of a raised shelf around the soliton with height on either side given by

$$h^\pm = \frac{u_\infty \pm A}{2u_\infty B}. \tag{40}$$

Note that $\alpha(Z) > 0$, so the shelf persists for all Z. From (33), the prediction for the soliton phase is then

$$\sigma_0(Z) = \frac{B(0)}{u_\infty(0)}Z + \sigma_0(0). \tag{41}$$

These predictions for the shelf height and evolution of the soliton phase are reproduced identically from the formulae (17c)–(17e). The soliton center t_0 is the only parameter for which the predictions obtained using the two approaches described in this work differ. In particular, the orthogonality condition (35) yields

$$t_0(Z) = \frac{A(0)}{2B(0)u_\infty(0)}(e^Z - 1) + t_0(0). \tag{42}$$

On the other hand, the prediction from the perturbed conservation laws approach comes in the form of a second-order differential equation, whose solution is

$$t_0(Z) = \frac{A(0)}{4B(0)u_\infty(0)}(3e^Z + e^{-Z} - 4) + t_0(0). \tag{43}$$

The two predictions both capture the small-Z behavior of the soliton center. Namely, their Taylor expansions agree up to $O(Z)$. However, since (43) is obtained using information at $O(\varepsilon^2)$, it is seen to remain valid for a larger interval in Z than (42). A direct comparison of (42) and (43) is shown in Figure 2 of [30].

It is also worth mentioning that in the case of a nonlinear damping perturbation,

$$F[u] = -i|u|^2 u, \tag{44}$$

the soliton parameters satisfy the following system of coupled nonlinear ordinary differential equations, which can be found using either method:

$$u_{\infty Z} = -u_\infty^3, \qquad A_Z = -\left(\frac{2}{3}A^2 + \frac{1}{3}u_\infty^2\right)A, \qquad B_Z = -\left(\frac{2}{3}A^2 + u_\infty^2\right)B. \tag{45}$$

It is straightforward to solve this system numerically. Additionally, we have

$$\alpha = 2B\left(\frac{2}{3}A^2 + \frac{5}{3}u_\infty^2\right), \tag{46}$$

which similarly indicates a raised shelf that persists for all Z.

4.2. Self-Steepening and Higher-Order Dispersion

For certain perturbations, the typical prominent radiation shelf may not develop around the dark soliton. From the perspective of the eigenfunction expansion approach, such cases correspond to those in which the singularities at $\zeta = \pm u_\infty$ in the first-order correction integral are removed, which is shown in [30] to occur when $\alpha = 0$, with α as in (31). This turns out to happen for a self-steepening perturbation of the form

$$F[u] = -i(|u|^2 u)_t. \tag{47}$$

For this perturbation we find that $u_{\infty Z} = A_Z = B_Z = 0$ and $\alpha = 0$ indicating that no shelf develops and $\sigma_{0Z} = 0$. Note that for any case where t_0 is the only parameter that evolves, the orthogonality condition (35) shows that its evolution is

$$t_{0Z} = -\frac{1}{2B^2}\int_{-\infty}^{\infty}\left\{\mathrm{Im}\big[(A - iB)F_0\big]e^{B\tau}\,\mathrm{sech}(B\tau) + AB\,\mathrm{Im}\,F_0\,\tau\,\mathrm{sech}^2(B\tau)\right\}d\tau. \tag{48}$$

Substituting the expression for F_0 in the self-steepening case gives

$$t_{0Z} = A^2 + u_\infty^2. \tag{49}$$

Thus, the shape of the soliton is perfectly preserved, but it experiences an acceleration effect as a result of the perturbation.

Another physically relevant perturbation under which a shelf is not predicted to develop is higher-order dispersion. Consider an arbitrary order ($n \geq 3$) dispersive perturbation of the form

$$F[u] = -(i\partial_t)^n u. \tag{50}$$

In this case, we have $u_{\infty Z} = 0$ and

$$A_Z = -\frac{B}{2}\,\mathrm{Im}\int_{-\infty}^{\infty} i^n \partial_\tau^n u_s(\tau)\,\mathrm{sech}^2(B\tau)d\tau. \tag{51}$$

Putting in the form of u_s one finds that if n is odd, then the integrand is purely real; and if n is even, then the integrand is an odd function of τ. In either case, we have that $A_Z = 0$, and in turn $B_Z = 0$. Also,

$$\alpha = -2\,\mathrm{Im}\int_{-\infty}^{\infty} u_s^*(\tau) i^n \partial_\tau^n u_s(\tau)d\tau, \tag{52}$$

which by a similar argument implies that $\alpha = 0$, i.e., no shelf develops for any dispersion order n.

4.3. Higher-Order Dissipation

Consider an arbitrary order ($n \geq 1$) dissipative perturbation,

$$F[u] = i\partial_t^{2n} u, \tag{53}$$

of which $F[u] = iu_{tt}$ (i.e., diffusion-type) is a special case. For any n, we have $u_{\infty Z} = 0$ and

$$A_Z = \frac{B}{2} \operatorname{Im} \int_{-\infty}^{\infty} i\partial_\tau^{2n} u_s(\tau) \operatorname{sech}^2(B\tau) d\tau = 0. \tag{54}$$

So, the background, velocity, and depth do not evolve. However, unlike higher-order dispersion, a shelf is generated as seen from

$$\alpha = 2B^3 \int_{-\infty}^{\infty} \tanh(B\tau)\partial_\tau^{2n-1} \operatorname{sech}^2(B\tau) d\tau \neq 0. \tag{55}$$

The integrand is an even function of τ, so this integral is not forced to vanish by parity—in contrast to the odd integrands encountered for the higher-order dispersion case, where one finds $\alpha = 0$. For each value of n that we have evaluated explicitly the integral is found to be nonzero. In particular, in the case $n = 1$, corresponding to the ordinary dissipative perturbation, the integral is found to be $-4/3$, which gives

$$\alpha = -\frac{8}{3} B^3, \tag{56}$$

and a depressed shelf with height on either side given by

$$h^\pm = -\frac{2B(u_\infty \pm A)}{3u_\infty}, \tag{57}$$

with α and $h^\pm$ constant (i.e., independent of Z).

4.4. Stimulated Raman Scattering

We now consider the dynamics of a dark soliton under the influence of the stimulated Raman scattering effect, described by the perturbation

$$F[u] = u(|u|^2)_t. \tag{58}$$

We again have $u_{\infty Z} = 0$, and in this case we compute

$$A_Z = \frac{B}{2} \operatorname{Im} \int_{-\infty}^{\infty} u_s(|u_s|^2)_\tau \operatorname{sech}^2(B\tau) d\tau = \frac{4}{15} B^4, \tag{59}$$

or equivalently,

$$A_Z = \frac{4}{15}(u_\infty^2 - A^2)^2, \tag{60}$$

which can be solved numerically. This shows that, unlike any of the previously mentioned perturbations, the soliton velocity is not necessarily sign-definite. Particularly, we have that A is a strictly increasing function of Z. As such, if $A(0) < 0$, the soliton begins by traveling to the left, halts at some instant Z_0, and then proceeds to travel to the right for all $Z > Z_0$. This phenomenon is illustrated in Figure 1, and a direct comparison is given showing that the formula (60) agrees well with numerical measurements. Note that on the other hand, if $A(0) \geq 0$, the soliton travels to the right for all Z. This in turn gives for the soliton depth,

$$B_Z = -\frac{4}{15} A(u_\infty^2 - A^2)^{3/2}. \tag{61}$$

In the situation depicted in Figure 1, we have that B increases while $A < 0$ and decreases while $A > 0$. At the turning point $Z = Z_0$, the gray soliton instantaneously becomes a black (maximum depth) soliton. Next, we find that

$$\alpha = -\frac{8}{15} A(u_\infty^2 - A^2)^{3/2}. \tag{62}$$

Note that if $A(Z_0) = 0$ then $\alpha(Z_0) = 0$, i.e., the shelf disappears at the instant that the soliton changes direction.

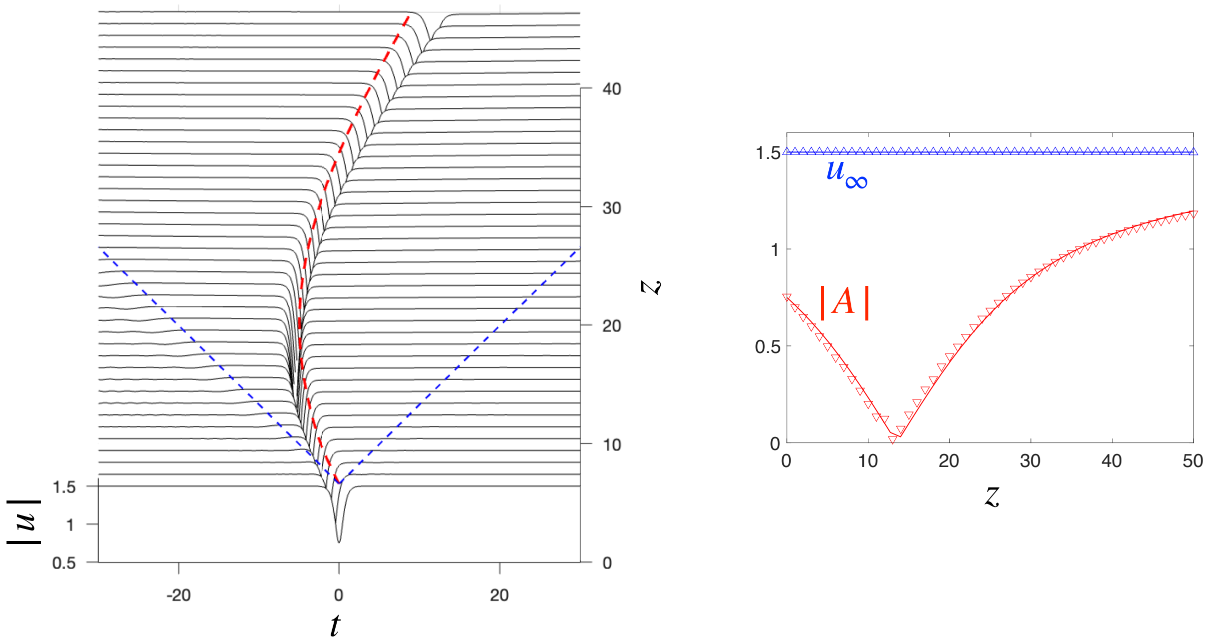

Figure 1. Left: Spacetime plot of the evolution of a dark soliton under the influence of the SRS perturbation with $u_\infty = 1.5$, $A(0) = -0.75$, $\varepsilon = 0.05$. With this (negative) initial velocity the soliton first travels to the left, momentarily becomes a black soliton at the turning point Z_0, and subsequently moves to the right, consistently with the monotone increase of $A(Z)$ predicted by (60). The red dashed line shows the predicted path of the soliton, while the blue dashed lines mark the edges of the shelf region. **Right**: Numerical measurements (triangles) of the background u_∞ and the trough amplitude $|A|$ (we plot the absolute value because A changes sign at Z_0) of the dark soliton compared to the analytical predictions (solid lines).

4.5. The Shelf and Conservation of Energy

While the first-order perturbation framework provides algebraic relations for the slow evolution of the soliton's core parameters, it is instructive to examine the shelf parameter α itself, and its fundamental connection to the macroscopic conserved quantities of the system.

As established in the derivation of the renormalized energy balance, the rate of change of the dark soliton's energy E (see (12a)), is explicitly tied to the shelf parameter. Indeed, the following relationship holds between the energy loss and the shelf parameter α:

$$E_Z = -(\alpha - 2B_Z). \tag{63}$$

Equation (63) captures the physical intuition that the continuous change in the soliton's energy must be perfectly balanced by the evolution of its depth and the mass symmetrically radiated into the asymptotic shelves. In particular, an implication of the above relationship is that for any perturbation that preserves conservation of energy (e.g., SRS), any change to the soliton's depth (B_Z) must be balanced by a shelf (α). On the other hand, for non-conservative perturbations, a shelf must emerge if the depth of the soliton is preserved (e.g., dissipation).

It is important to emphasize that the renormalized energy E is unique among the conserved quantities in its direct, algebraic coupling to α. By evaluating the remaining perturbed conservation laws, we find that they are fundamentally decoupled from the shelf parameter at leading order.

Consider the perturbed momentum balance, which evaluates the evolution of I (see (12b)). While the balance equation does incorporate boundary flux terms emanating from the asymptotic limits of the shelf, the symmetric nature of the shelf emission implies that these fluxes perfectly cancel one another. Because the generation of the shelf, quantified by α, represents a purely symmetric radiation of amplitude away from the soliton core, it carries zero net momentum. Consequently, α algebraically vanishes from the momentum balance, leaving the evolution of the momentum entirely independent of the shelf generation parameter.

Similarly, the Hamiltonian balance, derived from H (see (12d)), dictates the leading-order evolution of the soliton's velocity parameter, A_Z. Strikingly, no asymptotic boundary terms from the shelf appear at this order in the Hamiltonian evolution equation. Because the leading-order balance is driven purely by the localized interaction between the perturbation and the soliton core, it is completely insensitive to the mass dumped into the extending shelves, thereby rendering H_Z entirely decoupled from α.

Finally, the center of energy R (see (12c)), presents a unique challenge within the conservation laws framework.

Unlike the energy and momentum balances, the integrals defining the center of energy involve an explicit factor of the coordinate t. This unbounded algebraic growth causes the integrals to rigorously diverge when evaluated over the non-decaying, plateau-like shelf limits. As a result, these integrals fail to regularize under the simple asymptotic shelf approximations. To properly evaluate the positional shift of the soliton, one cannot rely on the macroscopic boundary fluxes; instead, one must work directly with the complete, nonlocal first-order correction, u_1. Therefore, no elementary algebraic connection can be established between the evolution of the center of energy and the macroscopic shelf parameter α.

Here, we apply the above arguments to some of the examples of physically relevant perturbations we considered in this Section.

- In the case of linear damping we have $\alpha = 2B$ and $B_Z = -B$, so $E_Z = -4B < 0$, corresponding to a loss of energy resulting from both a decrease in depth and a raised shelf.
- In the case of dissipation, we have $\alpha = -\frac{8}{3}B^3$ and $B_Z = 0$, so $E_Z = \frac{8}{3}B^3 > 0$, corresponding to a gain in energy. Since the soliton depth does not change, this gain in energy must be due to a *depressed* shelf, which we illustrate in Figure 2 along with numerical measurements of the renormalized energy.
- In a case of self-steepening or higher-order dispersion, we have $\alpha = 0$ and $B_Z = 0$, so $E_Z = 0$, consistently with the fact that the background and depth do not evolve and there is no shelf.
- In the case of Raman scattering, we have $\alpha = 2B_Z$, which implies that $E_Z = 0$, i.e., conservation of energy is preserved due a balance between the decrease in the depth of the soliton and the shelf.

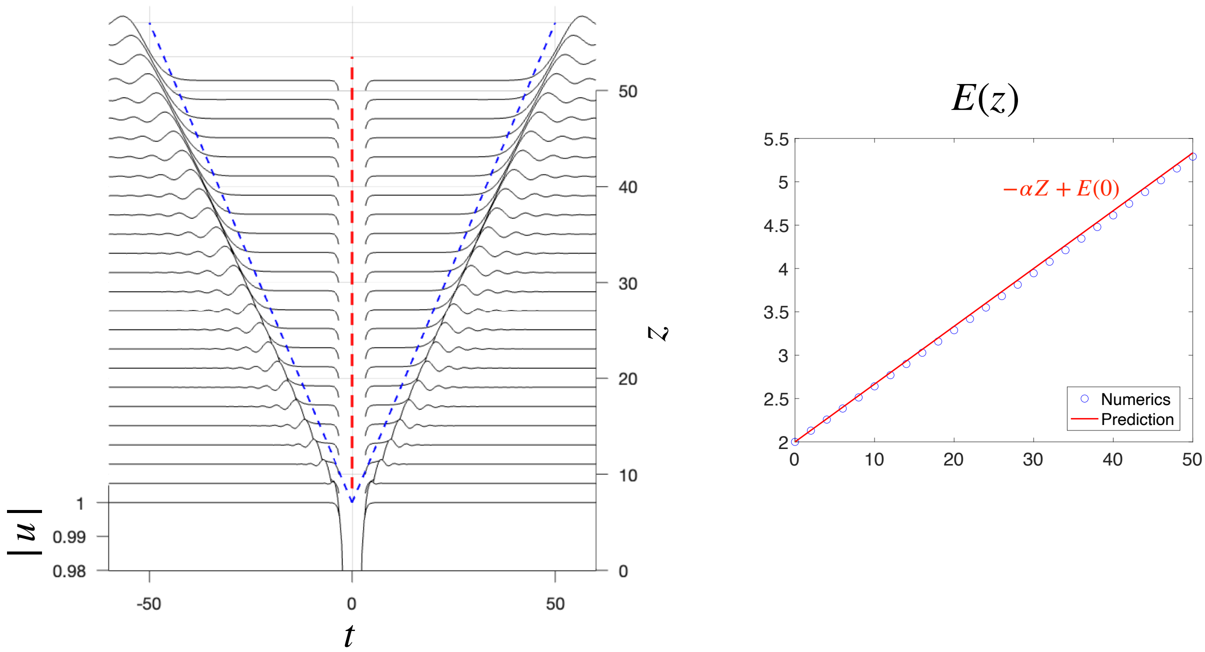

Figure 2. Left: Development of a depressed shelf around a black soliton ($A = 0$) with $u_\infty = B = 1$ under the influence of the dissipative perturbation $F[u] = iu_{tt}$ with $\varepsilon = 0.025$. **Right**: Numerical measurements (circles) of the renormalized energy E as a function of z compared with the analytical prediction (solid line). Note that since the depth of the soliton is preserved to leading order, the increase in the renormalized energy is due only to the shelf.

5. Conclusions

In this work, we have briefly presented and compared two complementary perturbative frameworks for analyzing the dynamics of dark solitons in the defocusing nonlinear Schrödinger (NLS) equation subject to small external perturbations. Our study is directly connected to the perturbation-induced dynamics of optical dark solitons governed by the NLS in the normal dispersion regime.

The first approach, based on perturbed conservation laws [27], provides a clean and efficient route to the evolution equations for the soliton parameters. By carefully regularizing the conserved quantities—energy, momentum, Hamiltonian, and center of energy—relative to the continuous-wave background, and by accounting for the moving boundaries of the expanding inner region through the fundamental theorem of calculus, one arrives at a closed algebraic system for the slowly varying parameters u_∞, A, B, and σ_0. The second approach, based on the linearization of the perturbed NLS equation and an eigenfunction expansion in terms of the squared Jost eigenfunctions of the associated inverse scattering problem [30], reproduces the same parameter evolution equations while additionally yielding an explicit, though involved, expression for the first-order correction. This expression is the key to characterizing the *shelf*: the plateau-like radiation field that generically surrounds the perturbed dark soliton, and which has no analogue in bright soliton perturbation theory (see, e.g., Ref. [11]).

On one hand, because the first-order correction fails to decay at infinity, standard Fredholm-type arguments on a fixed spatial domain are inapplicable; instead, the integral must be evaluated over an expanding inner region whose boundaries propagate at the speed of linear sound waves relative to the soliton core. Within the eigenfunction expansion framework, the shelf emerges precisely from the simple poles of the first-order correction at $\zeta = \pm u_\infty$, i.e., the branch points of the continuous spectrum. The entire shelf structure is encoded, at leading order, in the single scalar parameter

$$\alpha = -i\left\langle \begin{bmatrix} u_s^* \\ u_s \end{bmatrix}, W \right\rangle,$$

which measures the net coupling of the perturbation to the soliton through the generalized discrete eigenmode. A shelf develops if and only if $\alpha \neq 0$.

A central and unifying result of this paper is the exact algebraic relationship between the shelf parameter and the renormalized soliton energy:

$$E_Z = -(\alpha - 2B_Z).$$

This relation captures, in a single equation, the physical bookkeeping of energy exchange in the perturbed system: any change in the soliton's renormalized energy must be balanced by the combination of shelf radiation (quantified by α) and the evolution of the soliton depth. Strikingly, the remaining macroscopic conserved quantities decouple from α at leading order. The momentum balance is made shelf-independent by the symmetric nature of the shelf emission; the Hamiltonian balance is dominated by the localized soliton-perturbation interaction and is insensitive to the shelf at this order; and the center of energy involves integrals that diverge when naively evaluated over the non-decaying shelf, requiring the full nonlocal first-order correction for a proper treatment. The energy is therefore unique among the conserved quantities in its direct algebraic relation to the shelf. The physical implications of this result were illustrated through several examples, including linear damping, higher-order dissipation, self-steepening, higher-order dispersion, and stimulated Raman scattering, each yielding a distinct value of α and a correspondingly distinct energy budget.

Regarding the accuracy of the predictions, the evolution equations for the background amplitude u_∞, soliton velocity A, and depth B are well-validated and remain accurate up to propagation distances of order $z \sim 1/\varepsilon$ and beyond, as confirmed numerically in [30]. The predictions for the soliton phase σ_0 and center t_0 are accurate at short distances but lose quantitative precision over longer scales; obtaining estimates that remain valid up to $z = O(1/\varepsilon)$ would require knowledge of the $O(\varepsilon^2)$ corrections to the amplitude and velocity, and constitutes an open problem.

Future directions include the extension of this framework to multi-soliton configurations, as well as dark-dark and dark-bright soliton pairs of the coupled defocusing NLS system, for which direct perturbation theories have recently been developed [32], and to non-integrable settings where the squared-eigenfunction basis is no longer available and alternative expansion strategies must be employed. Direct experimental implications in optical systems and Bose–Einstein condensates, particularly in regimes where perturbations preserve the renormalized energy while generating a nontrivial shelf, remain a compelling avenue for further investigation.

Regarding experimental relevance, we recall that the defocusing NLS equation governs envelope propagation in optical media with normal group-velocity dispersion and a self-defocusing (negative) Kerr nonlinearity. This regime is routinely accessible in standard single-mode silica fibers operating below the zero-dispersion wavelength, as well as in defocusing photorefractive crystals and thermal (self-defocusing) nonlinear media, in all of which dark and gray solitons have been observed [4–6, 8, 10]. The perturbations considered here are not artificial: linear damping models fiber attenuation; higher-order dispersion and dissipation capture, respectively, third-order chromatic dispersion and spectral filtering or two-photon absorption; self-steepening originates from the intensity dependence of the group velocity; and stimulated Raman scattering accounts for the intrapulse Raman response of the medium [9,10]. Beyond optics, the same defocusing NLS (Gross–Pitaevskii) description applies to repulsively interacting atomic Bose–Einstein condensates, where dark solitons and their dissipative dynamics have likewise been realized experimentally [16,17]. The shelf structure analyzed here should therefore be observable, in principle, as a low-amplitude plateau accompanying a perturbed dark soliton in any of these settings.

Author Contributions

N.J.O.: Conceptualization, Formal analysis, Investigation, Methodology, Software, Validation, Visualization, Writing—original draft, Writing—review & editing; D.J.F.: Conceptualization, Formal analysis, Investigation, Methodology, Supervision, Validation, Writing—original draft, Writing—review & editing; T.P.H.: Conceptualization, Formal analysis, Investigation, Methodology, Supervision, Validation, Writing—original draft, Writing—review & editing; B.P.: Conceptualization, Formal analysis, Investigation, Methodology, Supervision, Validation, Visualization, Writing—original draft, Writing—review & editing. All authors have read and agreed to the published version of the manuscript.

Funding

BP and NJO gratefully acknowledge partial support for this work from the NSF, under grant DMS-2406626. BP acknowledges the Fulbright Foundation in Greece and the Fulbright program, and the Mathematics Department of the University of Ioannina, Greece, for the kind hospitality.

Institutional Review Board Statement

Not applicable.

Informed Consent Statement

Not applicable.

Data Availability Statement

Not applicable.

Conflicts of Interest

The authors declare no conflict of interest.

Use of AI and AI-Assisted Technologies

No AI tools were utilized for this paper.

References

1. Zakharov, V.E.; Shabat, A.B. Interaction between solitons in a stable medium. *Sov. Phys. JETP.* **1973**, *37*, 823–828.
2. Tsuzuki, T. Nonlinear waves in the Pitaevskii-Gross equation. *J. Low Temp. Phys.* **1971**, *4*, 441–457. https://doi.org/10.1007/BF00628744.
3. Hasegawa, A.; Tappert, F. Transmission of stationary nonlinear optical pulses in dispersive dielectric fibers. II. Normal dispersion. *Appl. Phys. Lett.* **1973**, *23*, 171–172. https://doi.org/10.1063/1.1654847.
4. Emplit, E.; Hamaide, J.E.; Reynaud, E.; et al. Picosecond steps and dark pulses through nonlinear single-mode fibers. *Opt. Commun.* **1987**, *62*, 374–379. https://doi.org/10.1016/0030-4018(87)90003-4.
5. Krökel, D.; Halas, N.J.; Giuliani, G.; et al. Dark-pulse propagation in optical fibers. *Phys. Rev. Lett.* **1988**, *60*, 29–32. https://doi.org/10.1103/PhysRevLett.60.29.
6. Weiner, A.M.; Heritage, J.P.; Hawkins, R.J.; et al. Experimental observation of the fundamental dark soliton in optical fibers. *Phys. Rev. Lett.* **1988**, *61*, 2445–2448. https://doi.org/10.1103/PhysRevLett.61.2445.
7. Hasegawa, A.; Kodama, Y. *Solitons in Optical Communications*; Clarendon Press: Oxford, UK, 1995. https://doi.org/10.1093/oso/9780198565079.001.0001.
8. Kivshar, Yu.S.; Luther-Davies, B. Dark optical solitons: Physics and applications. *Phys. Rep.* **1998**, *298*, 81–197. https://doi.org/10.1016/S0370-1573(97)00073-2.
9. Agrawal, G.P. *Applications of Nonlinear Fiber Optics*; Academic: San Diego, CA, USA, 2008. https://doi.org/10.1016/B978-0-12-374302-2.X5001-3.
10. Kivshar, Yu.S.; Agrawal, G.P. *Optical Solitons: From Fibers to Photonic Crystals*; Academic Press: San Diego, CA, USA, 2003. https://doi.org/10.1016/B978-0-12-410590-4.X5000-1.
11. Kivshar, Yu.S.; Malomed, B.A. Dynamics of solitons in nearly integrable systems. *Rev. Mod. Phys.* **1989**, *61*, 763. https://doi.org/10.1103/RevModPhys.61.763.
12. Zhao, W.; Bourkoff, E. Propagation properties of dark solitons. *Opt. Lett.* **1989**, *14*, 703–705. https://doi.org/10.1364/OL.14.000703.
13. Giannini, J.A.; Joseph, R.I. The propagation of bright and dark solitons in lossy optical fibers. *IEEE J. Quantum Electron.* **1990**, *26*, 2109–2114. https://doi.org/10.1109/3.64346.
14. Lisak, M.; Anderson, D.; Malomed, B.A. Dissipative damping of dark solitons in optical fibers. *Opt. Lett.* **1991**, *16*, 1936–1937. https://doi.org/10.1364/OL.16.001936.
15. Kivshar, Yu.S.; Yang, X.P. Perturbation-induced dynamics of dark solitons. *Phys. Rev. E* **1994**, *49*, 1657–1670. https://doi.org/10.1103/PhysRevE.49.1657.
16. Frantzeskakis, D.J. Dark solitons in atomic Bose-Einstein condensates: from theory to experiments. *J. Phys. A Math. Theor.* **2010**, *43*, 213001. https://doi.org/10.1088/1751-8113/43/21/213001.

17. Kevrekidis, P.G.; Frantzeskakis, D.J.; Carretero-González, R. *The Defocusing Nonlinear Schrödinger Equation: From Dark Solitons to Vortices and Vortex Rings*; SIAM: Philadelphia, PA, USA, 2015. https://doi.org/10.1137/1.9781611973945.
18. Ablowitz, M.J.; Segur, H. *Solitons and the Inverse Scattering Transform*; SIAM: Philadelphia, PA, USA, 1981. https://doi.org/10.1137/1.9781611970883.
19. Konotop, V.V.; Vekslerchik, V.E. Direct perturbation-theory for dark solitons. *Phys. Rev. E* **1994**, *49*, 2397–2407. https://doi.org/10.1103/PhysRevE.49.2397.
20. Kaup, D.J. A perturbation expansion for the Zakharov-Shabat inverse scattering transform. *SIAM J. Appl. Math.* **1976**, *31*, 121–133. https://doi.org/10.1137/0131013.
21. Chen, X.-J.; Chen, Z.-D.; Huang, N.-N. A direct perturbation theory for dark solitons based on a complete set of the squared Jost solutions. *J. Phys. A Math. Gen.* **1998**, *31*, 6929–6947. https://doi.org/10.1088/0305-4470/31/33/005.
22. Chen, X.-J.; Chen, Z.-D. Dark optical solitons on influence of the self-steepening term. *Chin. Phys. Lett.* **1998**, *15*, 504–506.
23. Lashkin, V.M. Perturbation theory for dark solitons: Inverse scattering transform approach and radiative effects. *Phys. Rev. E* **2004**, *70*, 066620. https://doi.org/10.1103/PhysRevE.70.066620.
24. Ao, S.-M.; Yan, J.-R. A perturbation method for dark solitons based on a complete set of the squared Jost solutions. *J. Phys. A Math. Gen.* **2005**, *38*, 2399–2413. https://doi.org/10.1088/0305-4470/38/11/006.
25. Kodama, Y.; Ablowitz, M.J. Perturbations of solitons and solitary waves. *Stud. Appl. Math.* **1981**, *64*, 225–245. https://doi.org/10.1002/sapm1981643225.
26. Burtsev, S.; Camassa, R. Nonadiabatic dynamics of dark solitons. *J. Opt. Soc. Am. B* **1997**, *14*, 1782–1787. http://doi.org/10.1364/JOSAB.14.001782.
27. Ablowitz, M.J.; Nixon, S.D.; Horikis, T.P.; et al. Perturbations of dark solitons. *Proc. Roy. Soc. A* **2011**, *467*, 2597–2621. https://doi.org/10.1098/rspa.2010.0663.
28. Horikis, T.P.; Frantzeskakis, D.J. Dark solitons in the presence of higher-order effects. *Opt. Lett.* **2013**, *38*, 5098–5101. https://doi.org/10.1364/OL.38.005098.
29. Horikis, T.P. Dark soliton dynamics under the complex Ginzburg-Landau equation. *Chaos Solitions Fract.* **2015**, *77*, 94–100. https://doi.org/10.1016/j.chaos.2015.04.019.
30. Ossi, N.J.; Prinari, B.; Yang, J. Integrable perturbation theory for dark solitons of the defocusing nonlinear Schrödinger equation. *J. Nonlinear Waves* **2026**, *2*, e10. https://doi.org/10.1017/jnw.2026.10035.
31. Prinari, B. Inverse Scattering Transform for nonlinear Schrödinger system on a nontrivial background: A survey of classical results, new developments and future directions. *J. Nonlin. Math. Phys.* **2023**, *30*, 317–383. https://doi.org/10.1007/s44198-023-00120-w.
32. Chernyavskiy, A.; Frantzeskakis, D.J.; Horikis, T.P.; et al. Dark-bright soliton perturbation theory for the Manakov system. *Proc. Roy. Soc. A* **2025**, *481*, 20240082. https://doi.org/10.1098/rspa.2024.0082.